DINAME 2017 - Proceedings of the XVII International Symposium on Dynamic Problems of Mechanics
A. T. Fleury, D. A. Rade, P. R. G. Kurka (Editors), ABCM, São Sebastião, SP, Brazil, March 5-10, 2017

Modelling and simulation of the rolling dynamics of a tractor-trailer truck vehicle

Ricardo Sampaio[1], **Flávio Celso Trigo**[1]

[1]Escola Politécnica da Universidade de São Paulo, Av. Prof. Luciano Gualberto, Travessa 3, n°. 380, 05508-010, São Paulo/SP, ricsampa@gmail.com, trigo.flavio@usp.br

Abstract: In this work, a 6 degree-of-freedom analytical model that describes the rolling dynamics of an articulated heavy-duty vehicle composed by a tractive (tractor) unit and a trailer unit was developed and numerically simulated. The behaviour of a typical medium-duty truck-trailer set was evaluated in two common traffic manoeuvres, namely, performing a constant steering wheel angle curve and a change of direction, both at constant velocity (36 km/h). In the latter case, in order to simulate a sudden change, steering amplitude ranging from zero to 30 degrees was imposed to the front wheels through a step function during 2 seconds. Results of the first trial revealed that the tractor roll angle presents a peak of 2.6 degrees and achieves a steady value of 0.8 degree respectively at 4 and 20 seconds after the beginning of the manoeuvre. Roll angle amplitudes of the trailer, spanning from -0.015 to 0.023 degree (a negative value means the vehicle is leaning inwards at the curve), revealed an oscillatory characteristic, before reaching a stable value of $2.5x10^{-3}$ *degrees in about 15 seconds. In the second trial, roll angles of both tractor and trailer reach maximum values higher than those of the previous test (respectively 11.5 and -0.5 degrees); in addition, the oscillatory movement of the trailer was enhanced, since positive and negative roll angles alternated five times until both units return to a steady (zero roll angle) condition after about 20 seconds from the beginning of the manoeuvre. Those results are compatible with the expected behaviour of actual vehicles, thus suggesting that the proposed model can be tailored to include other truck-trailer configurations and manoeuvres.*

Keywords: lateral dynamics, vehicle dynamics, roll dynamics, multibody system dynamics

INTRODUCTION

Truck vehicles play an important role in current freight transportation networks. Particularly in Brazil, according to data from 2008 (Lopes *et al*, 2008), road vehicles are used to carry 58% of the total amount of freights. A usual manner to enhance the load capacity of those vehicles is to employ a tractor unit to haul one or several trailer and/or semi-trailer units. The difference between a trailer and a semi-trailer is related to the kind of coupling between the hauled units to the towing vehicle and among themselves. When the coupling allows transferring part of the load from the hauled unit to the tractor or to another hauled unit (normally, through the coupling of a fifth wheel on the tractor and a device called kingpin on the hauled unit, see Fig. 1 and Fig. 2), the towed unit is called a semi-trailer; otherwise, it is a trailer. A consequence of the previous definition is that trailers have at least two axles. A typical 3-axle trailer is shown in Fig. 3. However, regardless of the kind of coupling, those vehicles are known as articulated trucks.

Due to their weight and dimensions, articulated trucks are prone to present dynamical instability even at normal operating conditions, i.e., forward travel at constant speed. Those instabilities may be caused by small perturbations on track (holes, bumps, sudden friction changes, uneven surfaces) or natural causes, such as wind gusts, that may lead to the potentially dangerous situations of jack-knifing, trailer swing, truck/trailer rollover, and flutter (Vieira, 2010). One of the possible outcomes of the above-cited situations is the rolling of the trailer/semi-trailer, tractor or of both. In the literature, there are two main sets of models that attempt to describe and predict the dynamical behaviour of articulated trucks, mostly for the purpose of supporting the design of passive or active control systems capable of avoiding unstable conditions: The ones whose equations of motion are obtained directly from the application of the theorems of mechanics (Chen and Tomizuka, 2000; Gäfvert and Lindgärde, 2004; Luijten, 2010), and those that rely on multibody dynamics simulation software, in which the whole model is numerically built and evaluated as, for instance, the work by Zhou and Zhang (2013).

To this end, a common feature of purely theoretical models is the use of simplifying hypotheses such as jack-knifing does not imply in rolling (Luijten, 2010), or identical roll angles of tractor and trailer (Chen and Tomizuka, 2000; Gäfvert and Lindgärde, 2004). On the other hand, multibody numerical models such as that from Zhou and Zhang (2013), despite considering several degrees of freedom and handling both holonomic and non-holonomic constraints, may represent a challenge for the control designer, given the universe of possible parameter combinations.

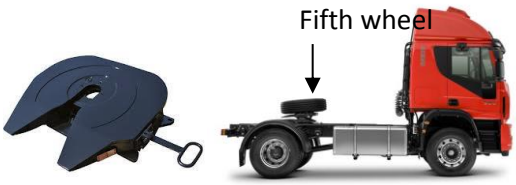

Figure 1 – Fifth wheel and tractor truck (Copeza, 2016; Iveco, 2016)

Figure 2 – Kingpin and semi-trailer (Corpesa, 2016; Rodoclara, 2016)

Figure 3 – Trailer unit (Rodocentroms, 2016)

Considering the above rationale, the present work aims at the development of a 6-degree-of-freedom analytical model to describe the rolling dynamics of an articulated tractor-trailer vehicle, and evaluating its performance through numerical simulations in two standard traffic manoeuvres, namely, constant radius curve and sudden change in direction maneuver, both at constant velocity. The proposed approach poses a contribution since, unlike Chen and Tomizuka (2000), Gäfvert and Lindgärde (2004) and Luijten (2010), the rolling of each unit is considered as a separate degree-of-freedom, thus allowing one to evaluate the dynamical interaction between trailer and tractor under normal or perturbed operational conditions.

MATERIALS AND METHODS

This section aims at presenting the theoretical background and the hypotheses used in the development of the analytical model of the vehicles. Firstly, only the tractor was considered, in order to qualitatively check the adequacy of the adopted hypotheses, especially those concerning tyre models. As the results were satisfactory, with physical responses consistent with the proposed manoeuvres, the model was extended to the entire vehicle, taking into account the trailer unit. All simulations were performed with the assistance of Matlab (R2012a version) and Mathematica (version 9.0).

Tractor vehicle model

The model to be developed is based on Chen and Tomizuka's (2000) box truck (Fig. 4), which is adapted to haul a trailer unit.

Figure 4 – Box truck (Iveco, 2015)

Equations of motion are obtained through the Lagrangean formalism (Greenwood, 1997), and they include tractor roll and yaw. A schematic representation of the vehicle, as well as the reference frames and their coordinate systems used in the development of the model, are shown in Fig. 5. The system Σ_t is rigidly attached to the unsprung element of the vehicle in such a way that the unit vector $\vec{t}_1$ is on the rolling axis, and that the direction of $\vec{t}_3$ intercepts the vehicle center of mass. On the other hand, Σ_s is fixed to centre of mass (sprung mass), with axes initially parallel with those of system Σ_t. Finally, Σ_n is the inertial reference frame.

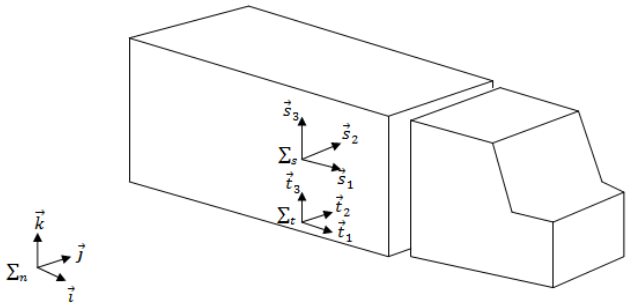

Figure 4 – Box truck (tractor vehicle) and reference frames

The three systems of coordinates are related by transformation equations (1) and (2), in which the functions sine and cosine are respectively represented by $s(x)$ and $c(x)$.

$$\{\vec{n}\} = \begin{pmatrix} c(\varphi) & -s(\varphi) & 0 \\ s(\varphi) & c(\varphi) & 0 \\ 0 & 0 & 1 \end{pmatrix} \{\vec{t}\} \tag{1}$$

$$\{\vec{t}\} = \begin{pmatrix} 1 & 0 & 0 \\ 0 & 1 & -\theta \\ 0 & \theta & 1 \end{pmatrix} \{\vec{s}\} \tag{2}$$

In Eq. (1), φ stands for the yaw angle of the unsprung element in relation to the inertial reference frame, whereas θ is the rolling angle of the sprung mass as observed from the reference frame attached to the unsprung element. The hypothesis of small angular displacements ($sin(\theta) \approx \theta\,, cos(\theta) \approx 1$) was employed in Eq. (2). This way, it is possible to write expressions for the kinetic energy and potential function for the vehicle centre of mass (CM) in relation to the inertial reference frame. To begin with, one expresses the position of the CM in relation to the inertial reference frame:

$$\begin{aligned} &\vec{p}_{CM/n} = \vec{p}_{CM/t} + \vec{p}_{t/n} \\ &\vec{p}_{CM/n} = z\vec{t}_3 + h\vec{s}_3 + x_n\vec{\imath} + y_n\vec{\jmath} \end{aligned} \tag{3}$$

In Eq. (3), x_n and y_n are the displacements of the origin of the unsprung element coordinate system in relation to the inertial reference frame, z is its height, and h is the height of the CM to the rolling axis. Differentiating Eq. (3) with respect to time, one obtains the velocity of the CM according to Eq. (4),

$$\{\vec{v}_{CG/n}\} = \begin{Bmatrix} (h\dot{\varphi}\theta + \dot{x}_n c(\varphi) + \dot{y}_n s(\varphi))\vec{s}_1 \\ (-h\dot{\theta} - \dot{x}_n s(\varphi) + \dot{y}_n c(\varphi))\vec{s}_2 \\ (\dot{x}_n \theta s(\varphi) - \dot{y}_n \theta c(\varphi))\vec{s}_3 \end{Bmatrix}, \tag{4}$$

in which the derivative of the unit vectors of the Σ_s base was calculated using the rotation vector of the sprung mass,

$$\vec{\Omega}_{s/n} = \dot{\theta}\vec{s}_1 + \dot{\varphi}\theta\vec{s}_2 + \dot{\varphi}\vec{s}_3.$$

The kinetic energy of the tractor unit can be than obtained through Eq. (5), where m_c (kg) is the mass and I (kg. m^2) is the central inertia tensor:

$$\begin{aligned} &T_c = \tfrac{1}{2} m_c \left(\vec{v}_{CM/n} \cdot \vec{v}_{CM/n}\right) + \tfrac{1}{2} \vec{\Omega}_{s/n} I \vec{\Omega^t}_{s/n} \Longrightarrow \\ &T_c = \tfrac{1}{2} m_c \left[\left(h\dot{\varphi}\theta + \dot{x}_n c(\varphi) + \dot{y}_n s(\varphi)\right)^2 + \left(-h\dot{\theta} - \dot{x}_n s(\varphi) + \dot{y}_n c(\varphi)\right)^2 + \left(\dot{x}_n \theta s(\varphi) - \dot{y}_n \theta c(\varphi)\right)^2 \right] + \\ &\tfrac{1}{2}(I_x \dot{\theta}^2 + I_y(\dot{\varphi}\theta)^2 + I_z \dot{\varphi}^2) \end{aligned} \tag{5}$$

The potential energy function, on the other hand, is given by Eq. (6), in which the hypothesis that the sprung mass swings about the vehicle rolling axis was considered:

$$V_c = m_c g h(c(\theta) - 1) \tag{6}$$

From equations (5) and (6), one writes the Lagrangean

$$L_c = T_c - V_c \tag{7}$$

and, through the Euler-Lagrange equations,

$$\frac{d}{dt}\left(\frac{\partial L}{\partial \dot{q}_i}\right) - \frac{\partial L}{\partial q_i} = Q_{q_i}, \quad i = 1, \dots, 4 \tag{8}$$

the equations of motion for the generalized coordinates $\boldsymbol{q} = [q_1, q_2, q_3, q_4]^T = [x_n, y_n, \theta, \varphi]^T$ and generalized non-conservative forces $\boldsymbol{Q} = \left[Q_{q_1}, Q_{q_2}, Q_{q_3}, Q_{q_4}\right]^T = \left[Q_x, Q_y, Q_\theta, Q_\varphi\right]^T$ associated to those coordinates can be written. In this model, the generalized non-conservative forces are those acting on the tyres, as depicted in Fig. 6, in which F_{lj} and F_{aj}, $j = 1, \dots 4$, respectively stand for the longitudinal and lateral forces. The forces acting at the suspension elements (orthogonal to the tyre forces, not shown in the figure) are represented by F_{sj}. For the computation of the non-conservative generalized forces, one first describes F_{lj}, F_{aj}, F_{sj} in coordinates of the Σ_n, as follows:

$$F_{xj} = F_{lj}c(\varphi) - F_{aj}s(\varphi) \tag{9}$$

$$F_{yj} = F_{lj}s(\varphi) + F_{aj}c(\varphi) \tag{10}$$

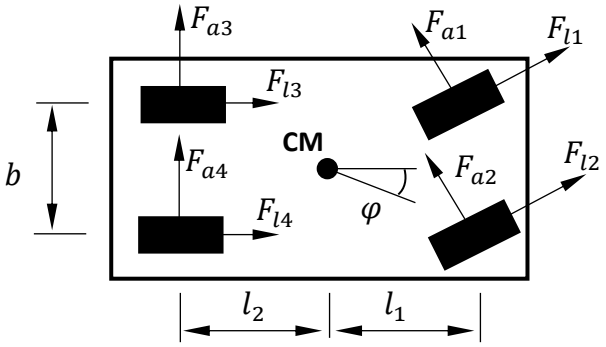

Figure 5 – Lateral and longitudinal forces at the tyres of the tractor truck

Since the scope of this work is the analysis of the lateral dynamics of the vehicle, all the manoeuvres are performed at constant velocity, i.e., $F_{lj} = 0, \ j = 1,2,3,4$. (Gillespie, 1992). Lateral forces, on the other hand, follow the model by Bareket & Fancher (1989), whose main assumption is that, at low speeds, their magnitude is proportional to the slip angle; moreover, the proportionality constant is the so called cornering stiffness (CS). The slip angles for tyres $j = 1, \dots, 4$ of Fig. 6 are given by Eqs. (11)-(14), in which δ represents the steering angle at the front tyres:

$$\alpha_1 = \delta - arctg\left(\frac{\dot{y}_t + l_1\dot{\varphi}}{\dot{x}_t - \frac{b}{2}\dot{\varphi}}\right) \tag{11}$$

$$\alpha_2 = \delta - arctg\left(\frac{\dot{y}_t + l_1\dot{\varphi}}{\dot{x}_t + \frac{b}{2}\dot{\varphi}}\right) \tag{12}$$

$$\alpha_3 = -arctg\left(\frac{\dot{y}_t - l_2\dot{\varphi}}{\dot{x}_t - \frac{b}{2}\dot{\varphi}}\right) \tag{13}$$

$$\alpha_4 = -arctg\left(\frac{\dot{y}_t - l_2\dot{\varphi}}{\dot{x}_t + \frac{b}{2}\dot{\varphi}}\right) \tag{14}$$

Another hypothesis that holds for low speeds is $arctg(x) \simeq x$; therefore, lateral forces are obtained by directly multiplying the slip angles and the CS, the latter admitted the same for all tyres. Suspension is modelled as a spring-viscous linear damping system. Thus,

$$F_s = k \cdot \epsilon + c \cdot \dot{\epsilon}, \tag{15}$$

with k representing spring stiffness and c denoting viscous damping coefficient, whereas ϵ stands for the displacement of the suspension, measured from the equilibrium position. Their values, for each tyre, are given by Eqs. (16)-(17).

$$\epsilon_1 = \epsilon_3 = -\frac{b}{2}\theta \tag{16}$$

$$\epsilon_2 = \epsilon_4 = \frac{b}{2}\theta \tag{17}$$

Given those hypotheses and constraints, the generalized forces, considered applied at points whose position is defined by vector $\vec{p}_j$ at each tyre $j,\ j = 1, \dots, 4$, are obtained according to Eq. (18).

$$Q_{q_i} = \sum_{j=1}^{4} F_{a_j} \frac{\partial(\vec{p}_j \cdot \vec{\imath})}{\partial q_i} + \sum_{j=1}^{4} F_{l_j} \frac{\partial(\vec{p}_j \cdot \vec{\jmath})}{\partial q_i} + \sum_{j=1}^{4} F_{s_j} \frac{\partial(\vec{p}_j \cdot \vec{k})}{\partial q_i},\ \ i = 1, \dots, 4. \tag{18}$$

Tractor and trailer vehicle model

In this section, an analytical model for the complete vehicle is developed. Its schematic representation is in Fig. (7), which includes reference frames Σ_U and Σ_r respectively fixed at the trailer rolling axis (unsprung element) and at the trailer sprung mass. Trailer attitude is described by the yaw angle, measured relatively to Σ_t, and by the roll angle, λ, of the trailer sprung mass, in relation to Σ_U. Rotation matrices among coordinate systems attached to reference frames Σ_U, Σ_r, and Σ_t are given by Eq. (19) and Eq. (20):

$$\{\vec{U}\} = \begin{pmatrix} c(\eta) & s(\eta) & 0 \\ -s(\eta) & c(\eta) & 0 \\ 0 & 0 & 1 \end{pmatrix} \{\vec{t}\} \tag{19}$$

$$\{\vec{r}\} = \begin{pmatrix} 1 & 0 & 0 \\ 0 & 1 & \lambda \\ 0 & -\lambda & 1 \end{pmatrix} \{\vec{U}\} \tag{20}$$

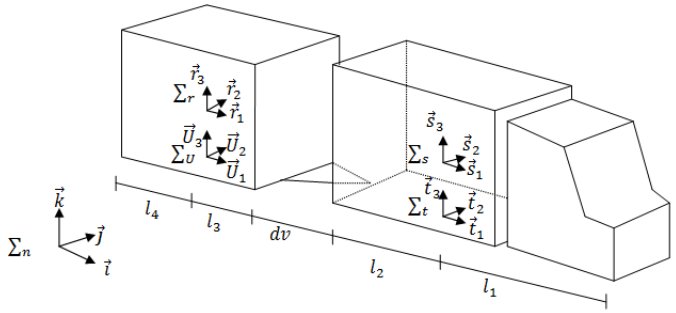

Figure 7 – Tractor and trailer vehicles and reference frames

In order to compute the kinetic energy of the trailer, one differentiates the position vector of its centre of mass, Eq. (21), with respect to time, thus obtaining Eq. (22):

$$\frac{d}{dt}(\vec{p}_{CG_2}) = \frac{d}{dt}(\vec{p}_{CG_1} - l_2\vec{s}_1 - h\vec{s}_3 - (dv + l_3)\vec{r}_1 + h_r\vec{r}_3) \tag{21}$$

$$\{\vec{v}_{CG_2}\} = \left\{ \begin{array}{c} \left(\begin{array}{c} \big(h\dot{\varphi}\theta + \dot{x}c(\varphi) + \dot{y}s(\varphi)\big)c(\eta) + \Big(-h\dot{\theta} - \dot{x}s(\varphi) + \dot{y}c(\varphi)\Big)s(\eta) + \\ \big(\dot{x}s(\varphi) - \dot{y}c(\varphi)\big)(-s(\eta)\theta^2) - -l_2\dot{\varphi}s(\eta) - l_2\dot{\varphi}\theta^2 s(\eta) - h\dot{\varphi}\theta c(\eta) + h\dot{\theta}s(\eta) + h_r\dot{\eta}\lambda \end{array} \right)\vec{r}_1 \\ \left(\begin{array}{c} \big(h\dot{\varphi}\theta + \dot{x}c(\varphi) + \dot{y}s(\varphi)\big)\big(-s(\eta)\big) + \Big(-h\dot{\theta} - \dot{x}s(\varphi) + \dot{y}c(\varphi)\Big)(c(\eta) + \theta\lambda) \\ +\big(\dot{x}s(\varphi) - \dot{y}c(\varphi)\big)(-\theta^2 c(\eta) + +\theta\lambda) - l_2\dot{\varphi}(c(\eta) + \theta\lambda) + l_2\dot{\varphi}\theta(-\theta c(\eta) + \lambda) + \\ +hs(\eta) + h\dot{\theta}(c(\eta) + \theta\lambda) - (dv + l_3)\dot{\eta} - h_r\dot{\lambda} \end{array} \right)\vec{r}_2 \\ \left(\begin{array}{c} \big(h\dot{\varphi}\theta + \dot{x}c(\varphi) + \dot{y}s(\varphi)\big)\big(\lambda s(\eta)\big) + \Big(-h\dot{\theta} - \dot{x}s(\varphi) + \dot{y}c(\varphi)\Big)(-\lambda c(\eta) + \theta) \\ +\big(\dot{x}s(\varphi) - \dot{y}c(\varphi)\big)(\theta^2\lambda c(\eta) + \theta) - l_2\dot{\varphi}(-\lambda c(\eta) + \theta) + l_2\dot{\varphi}\theta(\theta\lambda c(\eta) + 1) - \\ h\lambda s(\eta) + h\dot{\theta}(-\lambda c(\eta) + \theta) + (dv + l_3)\dot{\eta}\lambda \end{array} \right)\vec{r}_3 \end{array} \right\} \tag{22}$$

Furthermore, considering that m_r (kg) and I_r (kg. m^2) are the mass and the central inertia tensor of the trailer unit, its kinetic energy is written as

$$T_r = 0.5 m_r \vec{v}_{CG_2} \cdot \vec{v}_{CG_2} + 0.5 \vec{\Omega}_{s/n} I_r \overrightarrow{\Omega^t}_{s/n} \tag{23}$$

Under the same assumption of section "Tractor vehicle model", i. e., the sprung mass swings about the rolling axis, the potential energy of the trailer is

$$V_r = m_r g h_r (c(\lambda) - 1) \tag{24}$$

The last step to be taken before building the equations of motion for the whole vehicle concerns the determination of the non-conservative forces at the trailer tyres, as shown in Fig. 8, and the forces at the trailer suspension.

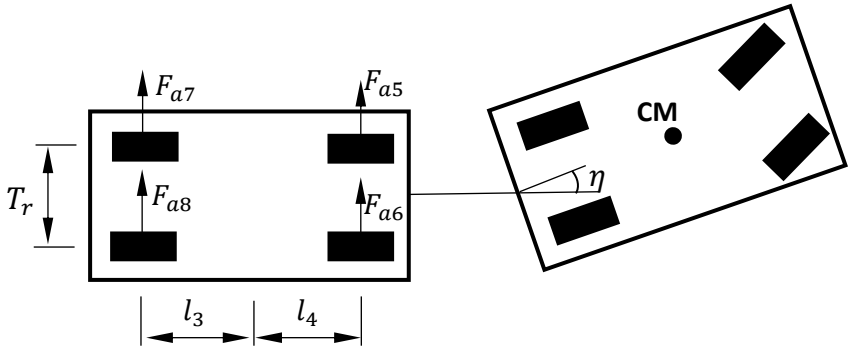

Figure 8 – lateral forces at the trailer tyres

Following the model proposed by Baraket & Fancher (1989) for the computation of forces at the tyres according to Eq. (9) and Eq. (10), briefly described in the previous section, the slip angles at low speeds can be approximated by Eq. (25):

$$\alpha_j = arctg\left(\frac{\vec{v}_j \cdot \vec{U}_2}{\vec{v}_j \cdot \vec{U}_1}\right), j = \{5,6,7,8\}\,, \tag{25}$$

in which $\vec{v}_j$ is the velocity of the trailer's $j-th$ tyre, in coordinates of the Σ_U frame, obtained by Eq. (26):

$$\begin{cases} \vec{v}_j = \vec{v}_U + \dot{\eta}\vec{U}_3 \wedge (\vec{p}_j - \vec{p}_U) \\ \vec{v}_U = \vec{v}_v + \dot{\eta} \wedge \vec{U}_3(-(dv + l_3)\vec{U}_1) \\ \vec{v}_v = \left(\dot{x}_n c(\varphi) + \dot{y}_n s(\varphi)\right)\vec{t}_1 + \left(-\dot{x}_n s(\varphi) + \dot{y}_n c(\varphi)\right)\vec{t}_2 + \dot{\varphi}\vec{t}_3 \wedge (-l_2\vec{t}_1) \end{cases} \tag{26}$$

Trailer suspension forces are calculated according to the linear spring-viscous damping model of Eq. (15), described in "Tractor vehicle model" section, as functions of the displacements

$$\epsilon_5 = \epsilon_7 = -\frac{b_r}{2}\lambda \tag{27}$$

$$\epsilon_6 = \epsilon_8 = \frac{b_r}{2}\lambda \tag{28}$$

Finally, the Lagrangean for the combined tractor-trailer vehicle can be written as

$$L = T_c + T_r - (V_c + V_r), \tag{29}$$

and the equations of motion follow from Eq. (8) for the vector of generalized coordinates $\boldsymbol{q} = [q_1, q_2, q_3, q_4, q_5, q_6]^T = [x_n, y_n, \theta, \varphi, \eta, \lambda]^T$, that includes the degrees of freedom from both units, and from Eq. (18), for the non-conservative generalized forces, with the summations $j = 1, \ldots, 8$, and $i = 1, \ldots, 6$. Both the algebraic derivation of the equations of motion and their simulation were performed with the aid of the software Mathematica.

RESULTS AND DISCUSSION

Firstly, the dynamic behaviour of the tractor unit without the trailer was evaluated in a simulated curve at constant $36\ km/h$ speed. In order to perform the manoeuvre, a constant steering angle of 4 degrees is imposed at the front wheels through a step function. Simulation parameters of a medium-weight commercial vehicle, given in Tab. 1, were obtained from Chen & Tomizuka (1997).

Results for this simulation are depicted in Fig. 9 and Fig. 10, from which it is possible to assert that the response of the dynamical model is coherent with the expected behaviour of a real vehicle in a similar manoeuvre. The initial gradient of the yaw rate (Fig. 9) is justified, since the vehicle is suddenly forced to detour from a straight line path until achieving a steady value ($d\varphi/dt \approx 15^o/s$), which corresponds to the constant steering input. The roll angle and roll rate (Fig. 10) are also compatible with the input condition: from the beginning of the manoeuvre, the vehicle leans outwards at the curve, as evidenced by the values of the roll angle θ, whereas, at the same time, roll rate $d\theta/dt$ presents oscillations that vanish once the steady condition is reached, at $\theta \approx 0.9$ degree, after about $20\ s$.

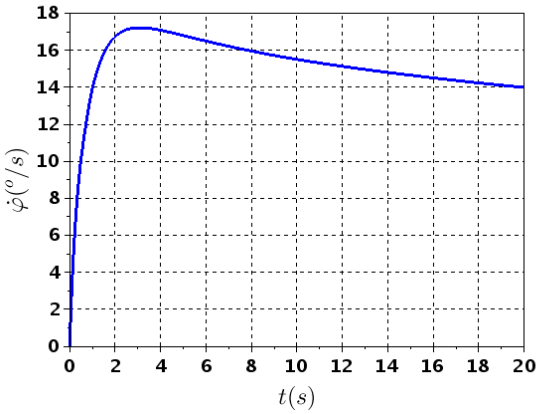

Figure 9 – Tractor yaw rate versus time for the constant steering wheel angle manoeuvre

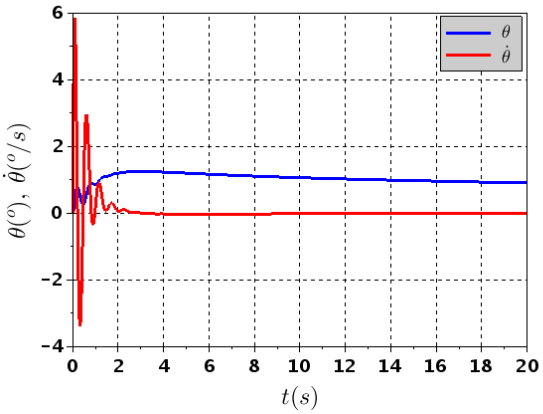

Figure 10 – Tractor roll angle and roll rate versus time for the constant steering wheel angle manoeuvre

Then, the dynamical response of the complete vehicle was obtained for two manoeuvres that frequently occur in normal traffic conditions, namely, performing a curve with the same characteristics as the one previously described, and a sudden change of direction from a straight line path, both at constant speed ($36\ km/h$). In the latter case, a 30-degree amplitude steering angle was imposed at the front wheels of the tractor through a step function. Parameters for this simulation can be found in Tab. 2, in which trailer values are identified by the "r" subscript. It is important to emphasize that some of those parameters, based in Chen & Tomizuka (2000), were adapted for the specific purposes of this work; they are marked with an asterisk.

Table 1 – Tractor vehicle parameters

Parameters	Values
m_c	$8400\ kg$
h	$0.5\ m$
z	$1.2\ m$
l_1	$2.5\ m$
l_2	$1.5\ m$
b	$2.0\ m$
Ix	$12447\ kg.m^2$
Iy	$65735\ kg.m^2$
Iz	$65735\ kg.m^2$
k	$5 \times 10^5\ N/m$
c	$9080\ N.s/m$
g	$9.8\ m/s^2$
CS	$14330\ N/rad$

Table 2 – Trailer vehicle parameters

Parameters	Values
m_r^*	$4200\ kg$
$h_r = h$	$0.5\ m$
$z_r = z$	$1.2\ m$
$l_3 = l_4$	$2.5\ m$
$b_r = b$	$2.0\ m$
Ix_r^*	$6624\ kg.m^2$
Iy_r^*	$32868\ kg.m^2$
Iz_r^*	$32868\ kg.m^2$
$k_r = k$	$5 \times 10^5\ N/m$
$c_r = c$	$9080\ N.s/m$
$CS_r = CS$	$14330\ N/rad$

Time evolutions of the tractor and trailer roll amplitudes for the constant steering wheel angle manoeuvre are depicted in Fig. 11 and Fig. 12. It is possible to realize that the trailer, constrained to the tractor unit, imposes an inertial resistance to the rolling tendency of the latter when the convoy achieves a steady condition. This assertion is corroborated by comparing results from Fig. 10 and Fig. 11. In Fig. 10, the steady roll angle for the tractor is $\theta \approx 0.9$ degree whereas, for the convoy, $\theta \approx 0.8$ degree. However, during the transient that follows the imposition of the step function, the tractor roll amplitude reaches a peak value of about 2.6 degrees (Fig. 11), against about 1.2 degree (Fig. 10) when the same vehicle was simulated without the trailer. The roll angle of the trailer initially accompanies the movement of the tractor and, due to the action of the suspension, oscillates during the transient phase until stabilizing after about $20s$., with the unit leaning outwards, as expected.

Results of the simulated sudden change of direction from a straight line path are depicted in Fig. 13 and Fig. 14. Although the step steering amplitude of 30 degrees was imposed during 2 seconds, starting at the abscissa $t = 3s.$ in Fig. 13, the whole convoy took about 20 seconds to fully stabilize at the new heading. The tractor leaning outwards and the trailer oscillating behaviour (Fig. 14) were compatible with the characteristics of the manoeuvre. It must be enhanced, though, that the peak of roll amplitudes of both vehicles, when compared to those obtained in the constant steering wheel angle condition, were considerably higher, namely, about 4 and 10 times, respectively for the tractor and trailer.

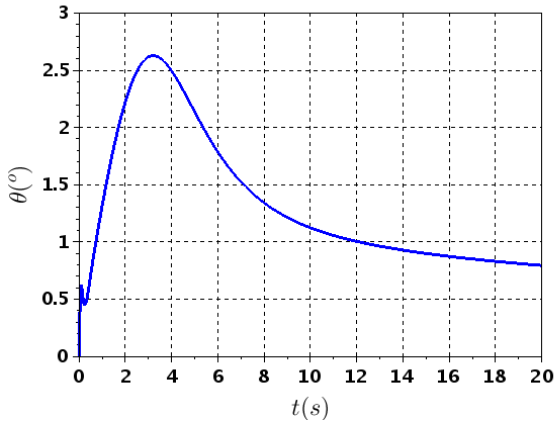

Figure 11 – Tractor roll angle versus time for the constant steering wheel angle manoeuvre

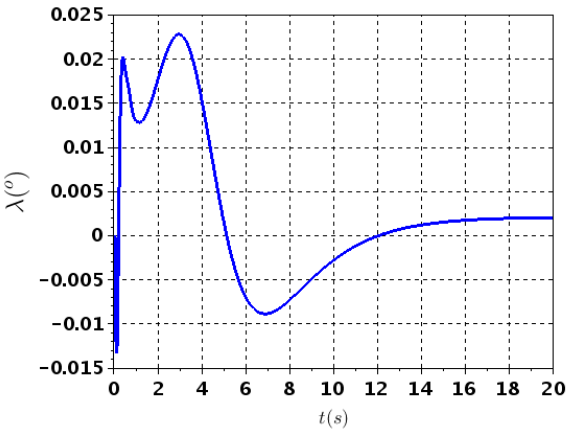

Figure 12 – Trailer roll angle versus time for the constant steering wheel angle manoeuvre

Likewise, it is possible to infer that the combined inertial effects of both units imposes a limiting condition on the safe operation of the convoy, since roll angle amplitude for the tractor unit alone (Fig. 10) was about $1/2$ times that of the same vehicle constrained to the trailer, as shown in Fig. 11. In practice, the maximum constant velocity at which the manoeuvres are performed must be smaller for the convoy, which is, again, a result that supports the behaviour of similar vehicles under actual driving conditions.

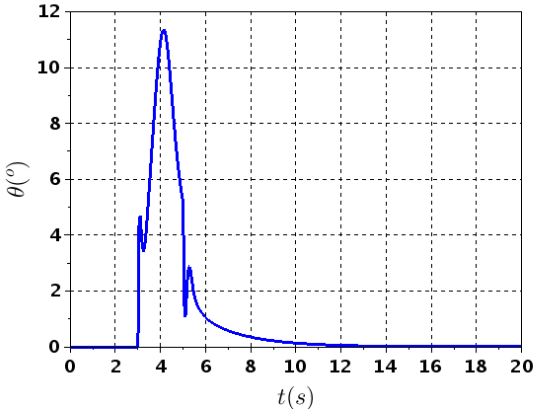

Figure 13 – Tractor roll angle versus time for the change of direction manoeuvre

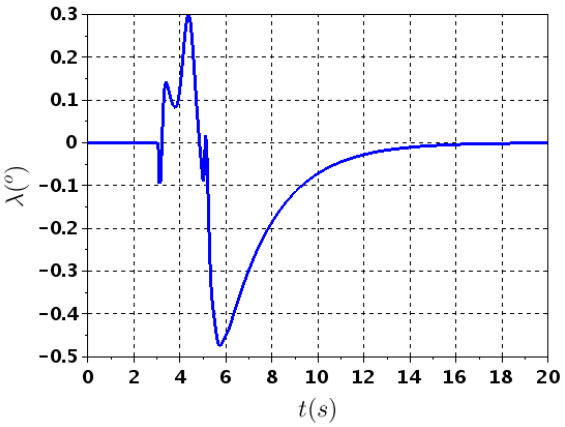

Figure 14 – Trailer roll angle versus time for the change of direction manoeuvre

CONCLUSIONS

In this work, a six-degree of freedom model of the rolling dynamics of a convoy vehicle was analytically obtained through the Lagrangean formalism. In order to cope with the complexity of the six nonlinear second-order coupled differential equation, the model was linearized for small rolling angles, thus helping its numerical integration. Still, simulated constant radius curve and sudden change of direction manoeuvres, both at constant velocity, exhibited results compatible to those observed in actual vehicles under similar operating conditions, thus stating the efficacy of the proposed model. Altogether, the transient response of the convoy evidenced the influence of the trailer on the behaviour of the tractor unit, since the peaks of roll amplitudes of the latter, especially in the change direction manoeuvre, were considerably higher, thus suggesting its susceptibility to experience unstable behaviour during that phase.

It should be pointed out that, due to the coherent results presented despite its simplicity, the model here developed might be used in parallel with some commercial multibody dynamics software in order to perform a cross-check on the outcomes of simulated conditions on convoy vehicles, since even recent publications rely solely on results provided by the above mentioned proprietary packages. Moreover, it is the intention of the authors to include combined effects of rolling and longitudinal dynamics (jackknife) in the analytical model and to analyse the overall stability, a key issue, for instance, in the development of active control systems.

REFERENCES

Banco Nacional de Desenvolvimento Econômico e Social, 2008. O transporte rodoviário de Carga e o Papel do BNDES, Brasil.

Baraket, Z. and Facnher, P., 1989, Representation of truck tire properties in braking and handling studies: The influence of pavement and tire conditions on frictional characteristics, UMITRI-89-33, University of Michigan,EUA.

Canale A.C. Alvarenga, G.S. and Viveros, H.P., 2009, Modelagem e análise de um veículo articulado utilizando a técnica dos multicorpos de Simmechanics em Matlab/Simulink®, Minerva 6(3), pp. 279-286..

Centro de Formação Profissional da Reparação Automóvel, 2007. Reboques, carroçamentos e equipamentos auxiliares, Lisboa, Portugal.

Chen C. and Tomizuka, M., 2000, Lateral Control of Commercial Heavy Vehicles. Vehicle System Dynamics, 33 , pp. 391–420.

Copeza. Indústria e Comércio de Peças Zanarotti Ltda. Available at www.copeza.com.br. Access on 2016/11/3.

Corpesacessorios. Corpes Acessórios e Peças Diesel. Available at www.corpesacessorios.com.br. Access on 2016/11/3.

Gäfvert, M. and Lindgärde, O., 2004, A 9-DOF Tractor-Semitrailer Dynamic Handling Model for Advanced Chassis Control Studies, Vehicle System Dynamics 41(1), pp. 51-82.

Gillespie, T.D. 1992, Fundamentals of vehicle dynamics, Society of Automotive Engineers, USA.

Greenwood, D.T. 1997, Classical Dynamics, Dover Books on Physics, USA.

Iveco. Available at www.iveco.com. Access on 2015/9/12.

Luijten, M.F.J., 2010, Lateral Dynamic Behaviour of Articulated Commercial Vehicles. Thesis (Master). Eidhoven University of Technology, Eidhoven, The Nederlands.

Pacejka H.B and Bakker, D.E, 1991, The Magic Formula Tire Model, Proceedings of 1st International Colloquium on Tire Models for Vehicles Dynamics Analysis. Delft, The Netherlands.

Rodocentro. Rodocentro Equipamentos Rodoviários. Available at www.rodocentroms.com.br. Access on 2016/11/3.

Rodoclara. Rodoclara Implementos Rodoviários. Available at www.rodoclara.com.br. Access on 2016/11/3.

Vieira J.L.M, 2010, Estudo de dirigibilidade de veículos longos combinados, Dissertação (Mestrado). Departamento de Engenharia Mecânica, EESC-USP, São Carlos, SP, Brasil.

Zhou, S. and Zhang S., 2013, Assessing the Effect of Chassis Torsional Stiffness on Tractor Semi-trailer Rollover, Applied Mathematics & Information Sciences 7 (2), pp. 633-637.

RESPONSIBILITY NOTICE

The authors are the only responsible for the material included in this paper.